



Contents lists available at ScienceDirect

Defence Technology

journal homepage: [www.elsevier.com/locate/dt](http://www.elsevier.com/locate/dt)

# Effect of wave shaper on reactive materials jet formation and its penetration performance

Huan-guo Guo, Yuan-feng Zheng, Le Tang, Qing-bo Yu, Chao Ge, Hai-fu Wang\*

Beijing Institute of Technology, China

## ARTICLE INFO

### Article history:

Received 21 January 2019  
Received in revised form  
20 April 2019  
Accepted 13 May 2019  
Available online xxx

### Keywords:

Shaped charge  
Reactive materials liner  
Wave shaper  
Reactive jet  
Penetration performance

## ABSTRACT

Wave shaper effect on formation behavior and penetration performance of reactive liner shaped charge (RLSC) are investigated by experiments and simulations. The reactive materials liner with a density of  $2.3 \text{ g/cm}^3$  is fabricated by cold pressing at a pressure of 300 MPa and sintering at a temperature of  $380^\circ\text{C}$ . Experiments of the RLSC with and without wave shaper against steel plates are carried out at standoffs of 0.5, 1.0, and 1.5 CD (charge diameter), respectively. The experimental results show that the penetration depths and structural damage effects of steel plates decrease with increasing the standoff, while the penetration depths and the damage effects of RLSC without wave shaper are much greater than that with wave shaper at the same standoff. To understand the unusual experimental results, numerical simulations based on AUTODYN-2D code are conducted to discuss the wave shaper effect, including the propagation behavior of detonation wave, the velocity and temperature distribution of reactive jet, and penetration depth of reactive jet. The simulations indicate that, compared with RLSC without wave shaper, there is a higher temperature produced inside reactive jet with wave shaper. This unusual temperature rise effects are likely to be an important mechanism to cause the initiation delay time of reactive jet to decline, which results in significantly decreasing its penetration performance.

© 2019 Published by Elsevier Ltd. This is an open access article under the CC BY-NC-ND license (<http://creativecommons.org/licenses/by-nc-nd/4.0/>).

## 1. Introduction

Reactive liner shaped charge (RLSC) is an extremely efficient demolition technology because of the unique performances, typically such as much greater behind-armor effectiveness and enhanced structural damage effects after penetrating [1]. RLSC produces an energetic material jet that releases its chemical energy within the target during or at the termination of the penetration process, resulting in dramatically catastrophic structural damage to concrete, masonry or geologic material targets [2,3], especially the excellent fragmentation effects of steel plates [4]. Due to the potential applications in shaped charge warheads, the reactive materials liner has been studied extensively and intensively in recent years. In general, the reactive liner materials are fabricated by introducing active metal powders into a polymer binder via a pressing/sintering process, typically such as Al/PTFE reactive materials [5–7]. The Johnson-Cook strength model of Al/PTFE was developed by the Split Hopkinson bar and quasi-static compression

experiments to study the formation behavior of reactive materials jet, which fitted well with that of X-ray tests [8,9]. The standoff effect experiments of RLSC illustrated that the excellent concrete damaging capability was greatly influenced by standoff, namely, the damaging capability was better in a region between 0.5 and 1.0 CD of standoff, but the demolition capability dropped off significantly at standoff 2.0 CD [10]. The damage mode and fragmentation mechanism of concrete and steel targets were not only influenced by the effective mass of reactive jet inside the penetration hole, but also remarkably affected by the initiation location of reactive jet. In other words, the terminal damage effects of RLSC will enhance with increasing the jet effective mass and penetration depth [4,11]. However, compared with the traditional metal jet, such as the copper jet and aluminum jet impacted steel targets by producing a deep penetration hole, whereas the reactive materials jet penetrating steel targets just produced a lower penetration hole. It is therefore extremely important to enhance the penetration performance of RLSC against steel targets.

Generally, a wave shaper can be actively inserted in the explosive of traditional metal liner shaped charge to adjust detonation wave shape, in order to increase the jet tip velocity and eventually improve the penetration performance and the terminal damage

\* Corresponding author.

E-mail address: [wanghf@bit.edu.cn](mailto:wanghf@bit.edu.cn) (H.-f. Wang).

Peer review under responsibility of China Ordnance Society

<https://doi.org/10.1016/j.dt.2019.05.005>

2214-9147/© 2019 Published by Elsevier Ltd. This is an open access article under the CC BY-NC-ND license (<http://creativecommons.org/licenses/by-nc-nd/4.0/>).

effects of shaped charges [12,13]. The methods of embedding a wave shaper into the charge have been employed and are still widely used in the traditional metal liner shaped charges [14–16]. An extreme overpressure zone [17] emerges at the top of the liner when a wave shaper is embedded in charge, which significantly enhances the high velocity impact between particles at axial line of liner, resulting in the temperature rise inside the liner. For the inert metal liner, the temperature rise can improve the ductility of the jet [18] and thus increase the penetration depth. However, for the reactive materials liner, high temperature may promote fast chemical reaction of reactive materials, which will cause more deflagration during jet formation and less deflagration inside the penetration hole [11].

In recent years, studies involving the shock induced chemistry of Al/PTFE [19–22], the combustion of Al/PTFE under high pressures and high strain rates [23–26], as well as high temperature induced reactive materials initiation [27,28] were widely conducted, by means of drop-weight test, ballistic impact, and differential scanning calorimetry (DSC) experiments and the like. It was obvious that, during shock load compression or intense dynamic loading, a temperature rise within reactive materials was resulted due to plastic deformation, jetting, and fracture. More importantly, the shock temperature was directly influenced by impact velocity (shock pressure), whereas the reaction rate and efficiency of reactive materials were significantly controlled by the temperature [22]. This phenomenon was observed from the experimental results obtained by Ames [23,24] which showed that the reaction efficiency increases with increasing the impact velocity, and it was also calculated that the initiation time of reactive materials after impact will drop with increasing the shock pressure. Baker [10] observed that high pressure inside reactive jet affected the damage effects of concrete targets. Moreover, Lee I. presented the PTFE will decompose at about 530 °C, at the same time, the micron-scale Al particles will participate in the reaction with the decomposition product of PTFE [27]. Dustin observed the violent exothermic reactions between the micron-Al and fluorinated gases at 600 °C around [28]. Hence, the temperature is a key parameter that can control the reaction behavior of reactive materials. It is well known that the jet velocity and temperature will increase when embedded a wave shaper in charge. However, the influence of temperature rise inside reactive jet on its formation and penetration performance of RLSC has not been well understood.

This paper begins with a series of RLSC penetrating steel plates experiments to investigate the effect of wave shaper on the penetration performance and structural damage effects. Subsequently, the propagation behavior of detonation wave, the velocity and temperature distribution of reactive jet are simulated. Finally, the effect of the temperature inside reactive jet on the initiation delay time and penetration performance is analyzed.

## 2. Experiments

### 2.1. Experiments of reactive liner shaped charge

#### 2.1.1. Reactive materials liner specimens

The processing method of the reactive materials liner would consist of four steps. Firstly, the reactive liner materials were the mixture of 73.5 wt% PTFE and 26.5 wt% Al powders by mass matched ratios. The average sizes of the PTFE and Al particles were approximate 100 and 44 μm, respectively. Secondly, putting a certain amount of the mixture powders into the pre-prepared mold, and then cold isostatic pressing the powders with a corresponding top mold at a high pressure. Again, sintering the pressed reactive liner specimens at a temperature of 380 °C in a vacuum oven. Lastly, the sintered reactive liners were reshaped to prevent

the liner deformation during the sintering process from affecting the jet formation. The prepared reactive liners are shown in Fig. 1. The experimental reactive liners were of the same shape and mass, with the base diameter of 66 mm, the wall thickness of 6.6 mm, and the cone angle of 60°.

#### 2.1.2. Experimental setup

In order to investigate the penetration performance of RLSC with and without wave shaper impacting steel plates, six experiments were carried out. Three of them were the RLSC with wave shaper, the rest tests were the RLSC without wave shaper. In addition to the wave shaper, the shaped charge consisted of a reactive liner, high-energy explosive, case and detonator, and the experimental setup is shown in Fig. 2. The height of main charge was 110 mm and the explosive was initiated by a detonator which was placed on the center of the charge. The boat tail case was machined by LY12 Aluminum with a thickness of 2 mm. The boat tail could reduce the main charge and the mass of the whole warhead, and maintain similar jet characteristics. The target plate was #45 steel cylinder with 120 mm in diameter and 100 mm in height.

#### 2.1.3. Experimental results of reactive liner

The experimental results are presented in Table 1. The results show that as the standoff increases, the penetration depth and the entrance hole diameter gradually decrease for the RLSC with wave shaper against steel plates. The largest penetration depth and entrance hole diameter occur at the standoff 0.5 CD, and the values are 0.7 and 0.68 CD, respectively. However, compared with the results of standoff 1.0 CD, the penetration depth and the entrance hole diameter decrease rapidly when standoff is 1.5 CD, reducing by about 47.5% and 36.2%, respectively.

Table 1 also shows that, when the standoffs are the same, the penetration depths and the entrance hole diameters of RLSC with wave shaper are all smaller than those without wave shaper. When the standoff is 0.5 CD, the RLSC without wave shaper has a maximum hole-diameter of 0.91 CD, which is about 25% larger than that with wave shaper. When the standoff is 1.0 CD, the penetration depth of RLSC with wave shaper is a slightly smaller than that without wave shaper, but the entrance hole diameter falls more than 37%. Especially, at the standoff 1.5 CD, the penetration depth drops off significantly, which declines about 58% of the RLSC without wave shaper. These indicate that the RLSC with wave shaper is more sensitive to standoff and its penetration capabilities dramatically reduce when standoff exceeds 1.0 CD.

Fig. 3 shows the damage effects of RLSC with wave shaper penetrating steel plates under different standoffs. When the



Fig. 1. Reactive liner specimens.

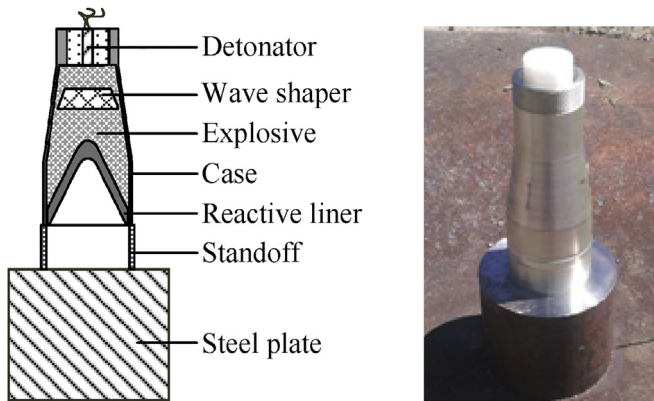


Fig. 2. Experimental setup.

standoff increases from 0.5 to 1.5 CD, there is no crack in the upper surface of the steel plate while some cracks occur in the inner surface of the penetration hole. Fig. 5 demonstrates the enhanced damage effects of RLSC without wave shaper. When the standoff is 0.5 CD, the steel plate is slightly broken up into two fragments and there are four cracks emanating from the hole under the combined effect of kinetic and chemical energy. When the standoff is 1.0 CD, four cracks are formed and three of them propagate throughout the steel plate upper surface, but there is no crack in the steel plate at 1.5 CD. Especially, the width of cracks near the inner surface of hole are larger, and the throughout cracks continue to propagate axially downwards from the upper surface of the plate. Moreover, it can also be seen from the test results that the penetration channel and the fracture surface are adhered by some black detonation products of reactive materials. It can be clearly observed that the upper surface of steel plate is almost completely covered by black detonation products.

In addition, it should be noted that the hole-diameter from the

surface of plate to the bottom of penetration hole is basically of the same widths under the smaller standoff (the left picture in Fig. 4 and Fig. 6). According to the experimental results, compared with the RLSC with wave shaper, an enhanced structural damage to the penetrated steel plate is produced by the RLSC without wave shaper at the standoff 0.5 and 1.0 CD. It indicates that the dramatically catastrophic damage effects of RLSC without wave shaper on steel plates strongly depend on the standoff.

## 2.2. Experiments of copper liner shaped charge

The above described structure and material of the wave shaper is a well-established technique that has been verified by experiments of copper liner. However, in order to better describe the problem, the contrast experiments of the copper liner shaped charge (CLSC) with and without wave shaper were carried out again. Except for the wall thickness of copper liner is 1.7 mm, the values of remaining dimensions are identical to ensure that its mass is the same as that of the reactive liner. Four experiments of copper liner were conducted, two of which were with wave shaper and two were without wave shaper. The experimental setup is shown in Fig. 7(1), and the typical results of CLSC with and without wave shaper impacting steel plates are shown in Fig. 7(2) and Fig. 7(3).

Based on the experimental results, with the standoff increasing from 1.0 to 1.5 CD, the penetration depths all increase significantly for CLSC with and without wave shaper (see Table 2). However, when the standoffs are 1.0 and 1.5 CD, the penetration depths of CLSC with wave shaper are always greater than that without wave shaper, increasing by about 15% and 20%, respectively. As such, a wave shaper is embedded in charge such that the way has been widely used in the traditional metal liner shaped charge warheads because the wave shaper can adjust the detonation wave to increase the jet tip velocity and eventually improve the penetration depth. Nevertheless, we found that the effect of wave shaper on the penetration behavior of RLSC against steel plates was significantly different from that of the CLSC.

Table 1

Experimental results of RLSC with and without wave shaper to steel plates.

Sequence	Standoff/CD	Wave shaper	Penetration depth/CD	Entrance hole-diameter/CD	Number of crack
1	0.5	Yes	0.77	0.68	No crack
2	1.0	Yes	0.61	0.58	No crack
3	1.5	Yes	0.32	0.37	No crack
4	0.5	No	0.79	0.91	Four cracks
5	1.0	No	0.73	0.84	Four cracks
6	1.5	No	0.76	0.59	No crack

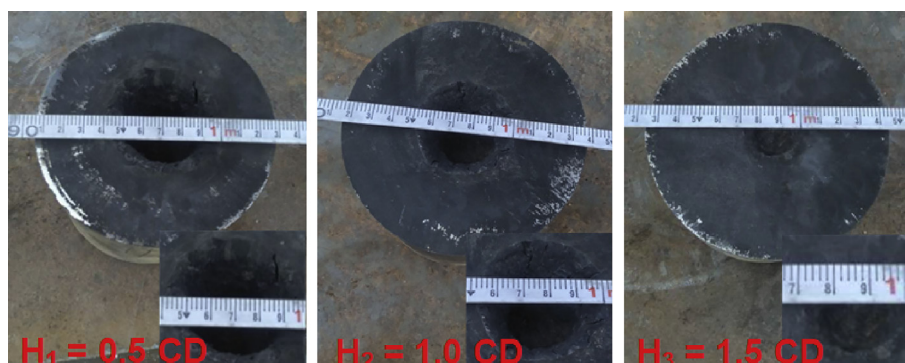


Fig. 3. Experimental results of RLSC with wave shaper.

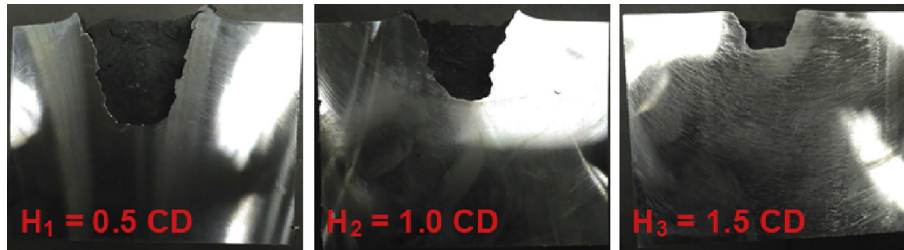


Fig. 4. Section views of RLSC with wave shaper.

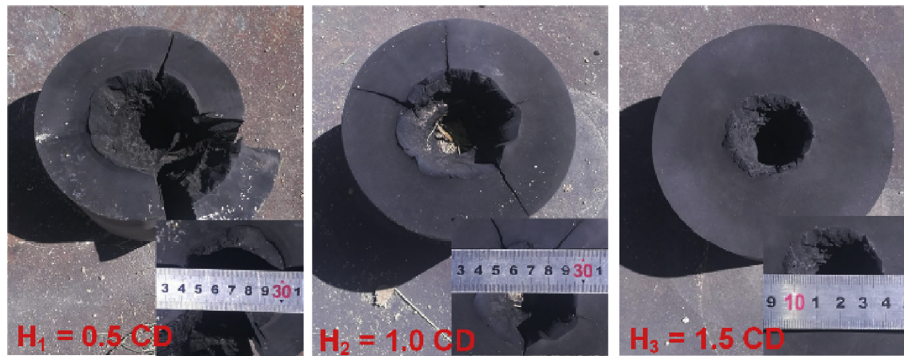


Fig. 5. Experimental results of RLSC without wave shaper.

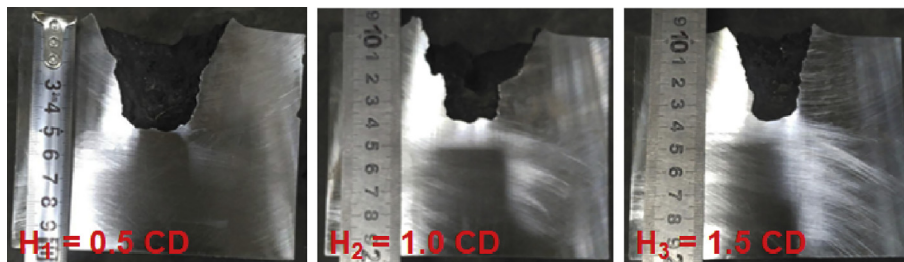


Fig. 6. Section views of RLSC without wave shaper.

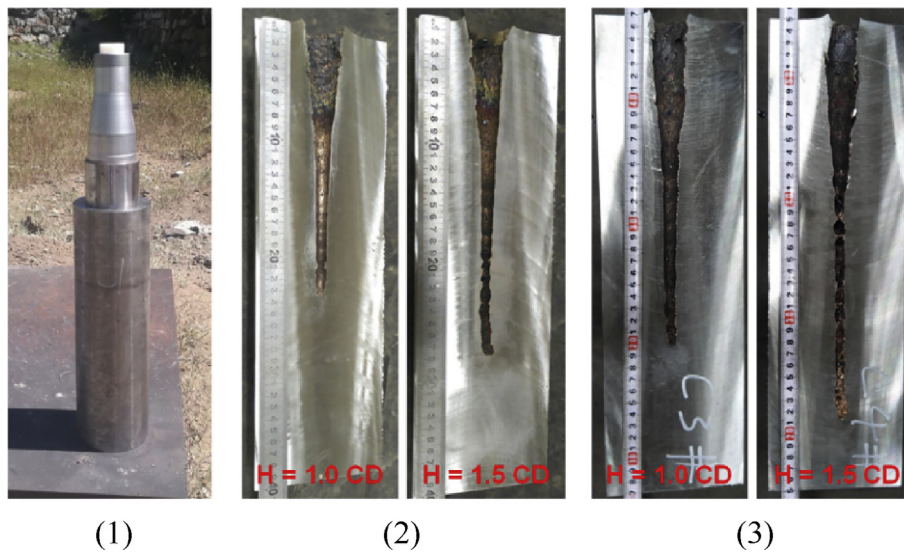


Fig. 7. Experimental setup and results (1) experimental setup (2) experimental results of CLSC without wave shaper (3) experimental results of CLSC with wave shaper.

**Table 2**  
Experimental results of RLSC against steel plates.

Sequence	Standoff/CD	Wave shaper	Penetration depth/CD	Entrance hole-diameter/CD
1	1.0	No	3.68	0.61
2	1.5	No	4.34	0.58
3	1.0	Yes	4.23	0.43
4	1.5	Yes	5.22	0.40

### 3. Analysis and discussion

To understand the unusual experimental results of RLSC with and without wave shaper against steel plates, numerical simulations based on AUTODYN-2D code are conducted to discuss the wave shaper effect on the propagation behavior of detonation wave, the velocity and temperature distribution of reactive jet, and further analyze the influence of temperature rise inside reactive jet on the initiation delay time of reactive jet and penetration performance.

#### 3.1. Numerical method and material model

In order to analyze the wave shaper effect on the jet formation and penetration performance of RLSC against steel plates, a Lagrange-Eulerian model was developed based on the platform of AUTODYN-2D code. The numerical geometrical parameters and the penetration schematic of RLSC are shown in Fig. 8 and Fig. 9, respectively. The explosive, case, wave shaper, and reactive liner were meshed by Eulerian algorithm to reduce the great deformation while the steel plate was meshed by Lagrangian algorithm for fracture and fragmentation. The mesh used a smaller size of  $0.5 \times 0.5$  mm per cell for the Euler domain of  $50 \times 500$  mm, and the mesh size of steel plate was  $1.0 \times 1.0$  mm. The boundary condition of air (Euler) domain was set as "Flow out (ALL EQUAL)" to eliminate the influence of the boundary effect.

The entire model of RLSC against steel plate mainly consists of six parts: air, liner, explosive, case, wave shaper, and steel target. Detailed material strength models and EOSs of RLSC each part are shown in Table 3.

The material parameters of air were derived from reference [18], and the main parameters are shown in Table 4, in which  $C_p$  and  $C_v$  are the specific heat at constant pressure and specific heat at constant volume, and  $E_0$  is the air in the specific energy.

The material of liner was reactive materials, and the reactive liner materials were modeled with a shock equation of state. The relation between the velocity  $U_s$  and the particle velocity  $u_p$  can be approximated by Ref. [8].

$$U_s = c_0 + Su_p \quad (1)$$

where  $c_0$  and  $S$  were based on data from plate-on-plate impact tests performed on the material. The Grüneisen parameter,  $\Gamma$ , was treated as a constant. The values for  $\Gamma$ ,  $c_0$ , and  $S$  in Table 5 were obtained from Taylor [8,29].

The reactive liner materials were described by the Johnson-Cook strength model, which expressed the behavior of materials subjected to high strains, high strain rates and high temperatures. This material model can be expressed as follows:

$$\sigma_y = [A + B(\bar{\epsilon}^p)^n] [1 + C \ln(\dot{\epsilon}^*)] \left[ 1 - \left( \frac{T - T_{room}}{T_m - T_{room}} \right)^m \right] \quad (2)$$

where  $A, B, C, M, N$  are material constants,  $\bar{\epsilon}^p$  is the effective plastic strain, and  $\dot{\epsilon}^*$  is the dimensionless strain rate.  $T_m$  is the melting temperature of the considered material,  $T$  and  $T_{room}$  are the surrounding and the room temperature, respectively.

The material of steel target was #45 steel, which was also chosen as the shock equation of state incorporating the Johnson-Cook strength model. The main parameters of reactive liner materials [8] and #45 steel [4] are shown in Table 5.

The choice of main charge is 8701 explosive, which material modeled by using the Jones-Wilkins-Lee (JWL) EOS. Table 6 represents the main parameters of 8701 [4].

The materials of wave shaper and case are EPOXY RES and Aluminum, respectively, which material parameters were derived from the material library in AUTODYN™ [30], as shown in Table 7.

#### 3.2. Detonation wave propagation behavior

The purpose of a wave shaper embedded in charge is mainly to adjust the shape of detonation wave front, control the direction of detonation wave propagation, and change the time of the detonation wave reaching the liner. Fig. 10 shows the propagation process of detonation wave in RLSC with and without wave shaper. It can be seen that the detonation wave of RLSC without wave shaper propagates with a spherical wave front centering on the detonation point along  $W_1$  (Fig. 10(1),  $t = 3 \mu s$ ). After initiation at  $5 \mu s$ , the detonation wave front reaches the top of the reactive liner, and the angle between the wave front and liner generatrix is  $\beta_1$ . However, for the RLSC with wave shaper, the propagation of detonation wave is divided into two paths (Fig. 10(2),  $t = 5 \mu s$ ). One path of detonation wave passes through the wave shaper to the reactive liner along  $W_1$ . Another path travels along  $W_2$  and  $W_3$ , which will superimpose after climbing the wave shaper to form an axisymmetric and convergent conical wave (Fig. 10(2),  $t = 8 \mu s$ ). The pressure at the superposition point rises sharply to form an extreme overpressure zone, and its pressure peak value can instantly reach 300 GPa. At this time, the detonation wave front reaches the top of the liner, and the angle between the wave front and liner generatrix is  $\beta_2$ . It is apparent that the angle  $\beta_2$  is less than  $\beta_1$ , so the initial impacting pressure on the surface of reactive liner with wave shaper is higher than that without wave shaper based on the Taylor formula [31]. As such, according to the momentum equation  $M dv/$

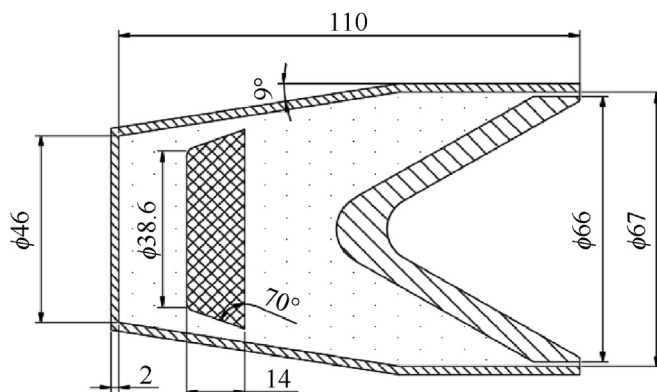


Fig. 8. Geometry (in mm) of RLSC with wave shaper.

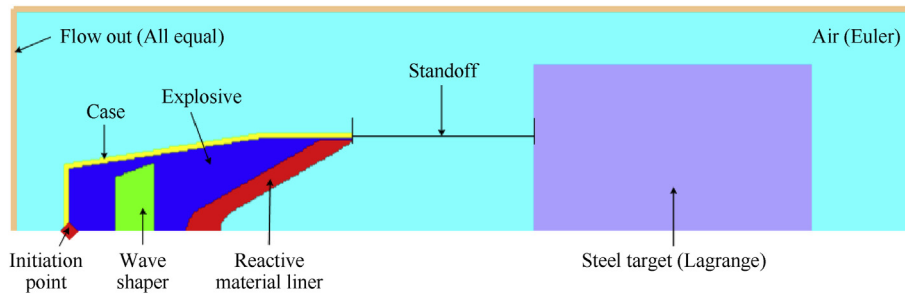


Fig. 9. Penetration schematic of RLSC against steel target.

Table 3 Material strength models and EOSs of RLSC each part.

Part	Materials	EOS	Strength model	Erosion
Air	Air	Ideal Gas	None	None
Liner	Reactive materials	Shock	Johnson Cook	None
Explosive	8701	JWL	None	None
Case	Aluminum	Shock	None	None
Wave shaper	EPOXY RES	Shock	None	None
Steel target	#45 steel	Shock	Johnson Cook	Geometric Strain 1.5

Table 4 Material parameters of air [18].

Material	$\rho/(\text{kg}\cdot\text{m}^{-3})$	$\gamma$	$C_p/(\text{kJ}\cdot\text{kg}^{-1}\cdot\text{K}^{-1})$	$C_v/(\text{kJ}\cdot\text{kg}^{-1}\cdot\text{K}^{-1})$	$T/\text{K}$	$E_0/(\text{kJ}\cdot\text{kg}^{-1})$
air	1.225	1.4	1.005	0.718	288.2	$2.068 \times 10^5$

Table 5 Parameters of the reactive liner materials and #45 steel materials.

Materials	$\rho/(\text{kg}\cdot\text{m}^{-3})$	$G/\text{GPa}$	$A/\text{MPa}$	$B/\text{MPa}$	$n$	$C$	$m$	$T_m/\text{K}$	$T_{\text{room}}/\text{K}$	$\Gamma$	$c_0/(\text{m}\cdot\text{s}^{-1})$	$S$
Reactive liner	2.27	0.67	8.04	250.6	1.80	0.400	1.00	500	294	0.90	1450	2.26
#45 steel	7.83	77.00	792.00	510.0	0.26	0.014	1.03	1793	300	2.17	4570	1.49

Table 6 Parameters of the explosive.

Material	$\rho/(\text{kg}\cdot\text{m}^{-3})$	$D/(\text{km}\cdot\text{s}^{-1})$	$P_{CJ}/\text{GPa}$	$e/\text{GPa}$	$A/\text{GPa}$	$B/\text{GPa}$	$R_1$	$R_2$	$\omega$	$v_0$
Explosive	1.71	8.315	28.6	8.499	524.23	7.678	4.2	1.1	0.34	1.00

Table 7 Parameters of the wave shaper and the case materials.

Materials	$\rho/(\text{kg}\cdot\text{m}^{-3})$	$\Gamma$	$C_I/(\text{m}\cdot\text{s}^{-1})$	$S_1$
EPOXY RES	1.186	1.13	2730	1.493
Aluminum	2.785	2.00	5328	1.338

$dt = SP$ , the compressive and closed speed of reactive liner element with wave shaper will increase with a higher initial impacting pressure. In addition, the overpressure detonation wave takes  $1 \mu\text{s}$  to completely pass through the top of the liner while the one without wave shaper takes  $2 \mu\text{s}$  to do the same thing. This phenomenon indicates that the time of the detonation wave acting on the liner dramatically decreases with increasing the pressure of detonation.

### 3.3. Reactive jet velocity distribution

Because the wave shaper causes the superposition of detonation wave to produce extreme overpressure zone, the impact pressure acting directly on the reactive liner is much higher than that without wave shaper. Moreover, based on the Gurney theory of explosive casting plates [32], when the angle  $\beta$  decreases, the detonation products behind the wave front will impact the liner at a higher speed, which further improves the compressive and closed speed of the reactive liner. Due to such two points, the wave shaper can improve the utilization of the explosive energy and thus advance the kinetic energy of the reactive jet, as shown in Fig. 11. For the RLSC with wave shaper, with increasing the kinetic energy, the tip velocity of reactive jet increases, resulting in decreasing the time of jet formation at the same standoff. Fig. 11 also verifies this phenomenon that the reactive jet formation time of RLSC without

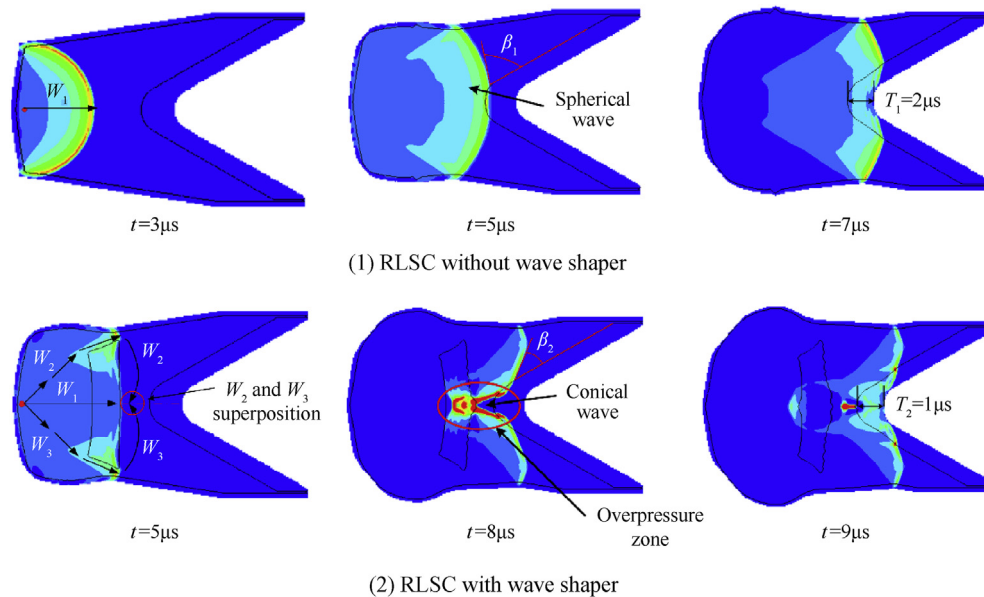


Fig. 10. Propagation behavior of detonation wave in explosive process.

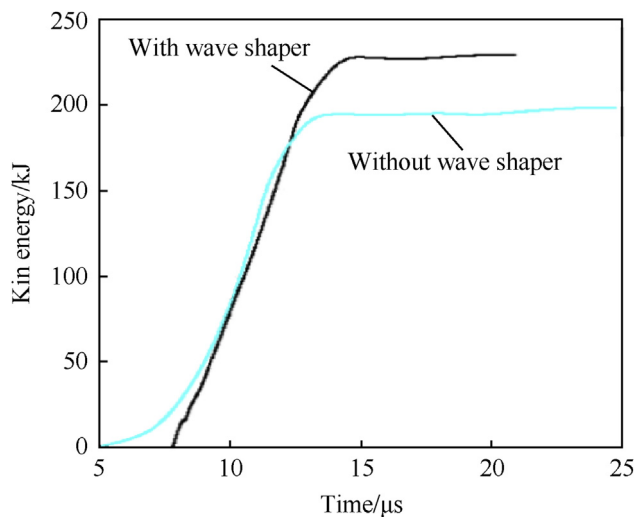


Fig. 11. Kin. Energy-time curves of reactive liner materials.

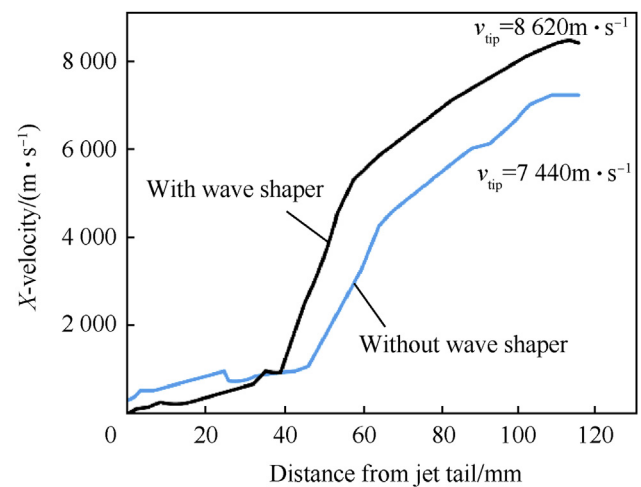


Fig. 12. Velocity distribution of reactive jet along the axis.

wave shaper is  $24.7 \mu\text{s}$  while RLSC with wave shaper is only  $20.9 \mu\text{s}$  at the standoff  $1.0 \text{ CD}$ . Also, it is obvious from Fig. 12 that the tip velocity of reactive jet with wave shaper is about 23.7% higher than that without wave shaper.

### 3.4. Reactive jet temperature distribution

Under the action of detonation wave, the reactive liner element obtains the compression and closed speed so that a shock wave inside the liner is formed. Due to the difference in the time of the shock wave action, the adiabatic shear deformation zone is produced in each section of reactive liner, and then the reactive liner materials are subjected to the action of the velocity inertia to make the large compression shear strain. The shear deformation of reactive liner mainly includes two parts, one is the adiabatic shear deformation of reactive liner along the vertical surface under the shock wave, and the other is the radial extrusion shear deformation belt formed by the reduction of reactive jet diameter during the

compression and closed process of liner. As such, the temperature rise inside reactive jet should be composed of two parts: 1) the temperature rise caused by the shock wave, 2) the temperature rise caused by the plastic deformation [33].

Fig. 13 and Fig. 14 show the temperature distribution of reactive jet with and without wave shaper at different standoffs, respectively, in which the black curve refers to the temperature values along the axis of reactive jet. Compared with reactive jet without wave shaper, there is a higher temperature produced inside reactive jet with wave shaper, especially that the temperature at the head and the rear parts of reactive jet exceed  $900 \text{ K}$  ( $900 \text{ K}$  is about the initiation threshold temperature of reactive liner materials [28]). This is mainly because when embedded a wave shaper in charge, the detonation waves superimpose at the top of reactive liner and produce an extreme overpressure zone, which will lead to the following two situations. Firstly, the peak value of shock wave pressure increases, which will directly cause the rise of temperature inside reactive jet [34]. Secondly, the compression and closed speed of the liner element increases, leading the plastic

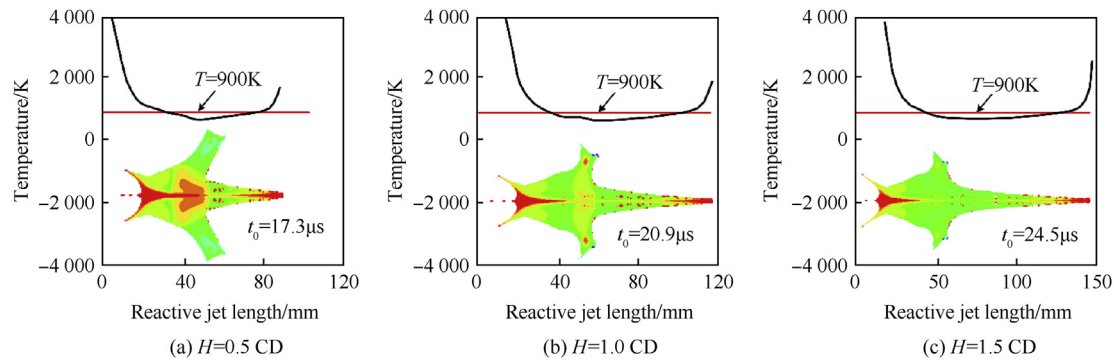


Fig. 13. Temperature distribution of reactive jet with wave shaper.

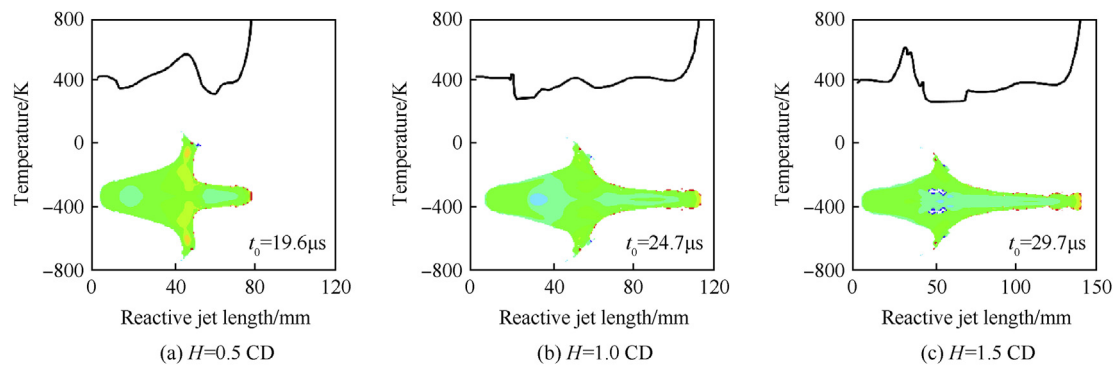


Fig. 14. Temperature distribution of reactive jet without wave shaper.

deformation of reactive liner to enhance, which will cause the rise of temperature inside reactive jet. However, for the reactive jet without wave shaper, the average temperature of the jet is relatively low, and its values are below 800 K (see in Fig. 14). In addition, it is very violent that the element at the interface between the jet and the slug collides during the initial stage of jet formation, causing the local high temperature at the interface, which will drop quickly as the jet elongation. Figs. 13 and 14 can verify this phenomenon that when the standoff increases from 0.5 to 1.5 CD, the temperature at the interface decreases gradually.

### 3.5. Reactive jet temperature effect on penetration performance

Under the high pressure of shock wave, the reactive liner produces high strain rate plastic deformation, which may activate the reactive liner materials. That is, the high-polymer PTFE molecules in the mixed powder materials will decompose, and the decomposition reaction releases fluoride with strong oxidation capability. As time passes, the metal powder Al rapidly undergoes a redox reaction with the fluoride, releasing a large number of high-temperature and high-pressure gas products and producing a significant deflagration effect [35]. The period of time from activation to initiation is called initiation delay time of reactive materials, during which assuming that reactive jet penetrates steel plate like metal jet. But when the time after activation reaches the initiation delay time, the reactive materials will rapidly have a deflagration reaction and the chemical energy would be immediately released, resulting in the reactive jet without the capability to continue to penetrate the target. As such, the reaction rate of reactive materials significantly influence on the initiation delay time. According to reference [22], the reaction rate and efficiency of reactive materials are significantly controlled by the temperature, so the temperature

is also likely important to affect the initiation delay time of reactive materials.

Reference [27] presented the PTFE will decompose at about 530 °C, at the same time, the micron-scale Al particles will participate in the redox reaction with the decomposition product of PTFE, resulting in about 65% mass loss of the mix powders. Therefore, for the reactive jet with wave shaper, the reactive materials of the jet head and rear parts may have a deflagration reaction during the stage of jet formation, so it may be the middle part of reactive jet that essentially contributes to the penetration capability. Based on the assumptions mentioned above, in order to more closely simulate the penetration performance of reactive jet with wave shaper against steel plates, the head part of jet that has undergone chemical reaction is deleted first (see in Fig. 15 (a)), and then the remaining jet penetrator is used to re-penetrate the steel plate (see in Fig. 15 (b)). However, as the average temperature of reactive jet without wave shaper is lower, it is assumed that the reactive jet chemical reaction will not occur before penetrating.

According to these two simulation methods, the penetration depth of reactive jet with and without wave shaper under different initiation delay time are shown in Fig. 16. Note that when the penetration depths of simulations are agreement with the experiments, the initiation delay time of reactive jet could be calculated. It is obvious that the initiation delay time with wave shaper is between 40 and 50  $\mu\text{s}$ , whereas the initiation delay time without wave shaper is between 70 and 80  $\mu\text{s}$ . The calculated results have also provided insight into the mechanism that the higher temperature or pressure [10] inside the reactive jet is likely important to increase the reaction rate of reactive materials and cause the initiation delay time of reactive jet to reduce. The conclusion also fits well with the experiments obtained by Ames which showed that the initiation time of reactive materials was inversely



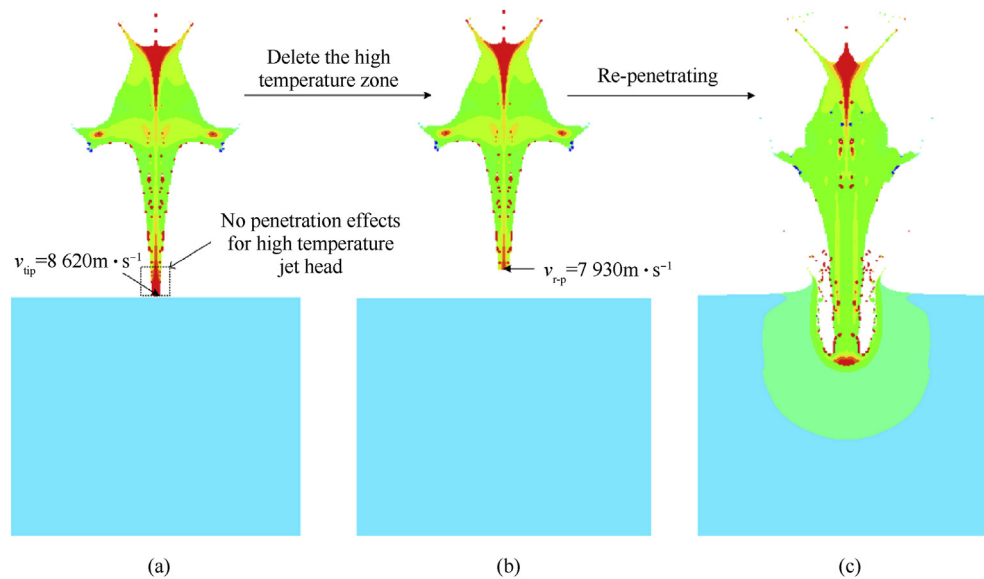


Fig. 15. Penetration process of reactive jet with wave shaper by simulations.

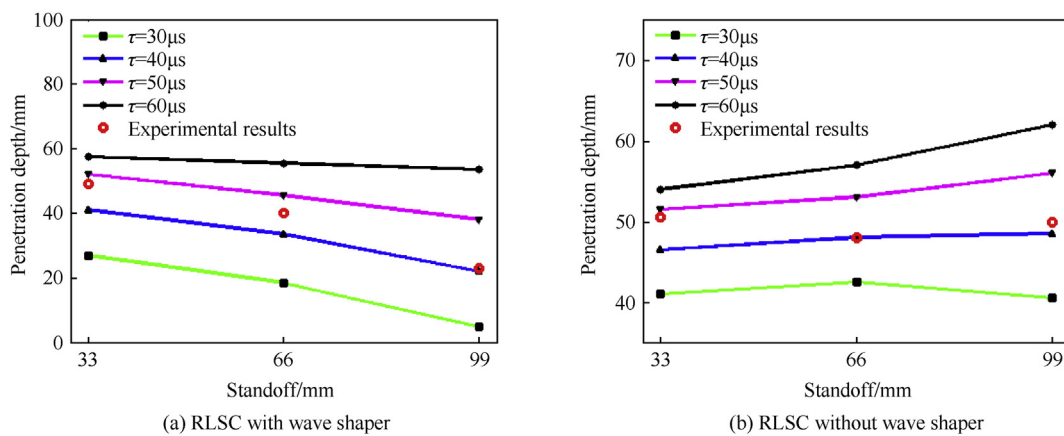


Fig. 16. Comparison of experimental and numerical penetration depths.

proportion to the initiation threshold stress [23]. Moreover, the numerical results also demonstrate that, for RLSC with or without wave shaper, the penetration depths increase markedly with increasing the initiation delay time under given conditions of standoffs and targets. However, when the initiation delay time is identical, namely,  $\tau = 60 \mu s$ , the penetration depths of RLSC with wave shaper are much larger than that without wave shaper. This phenomenon indicates that, if the initiation delay time is sufficiently long, a positive effect of wave shaper on penetration performance of RLSC is similar to the traditional metal liner shaped charge due to the increased jet tip velocity. Though the higher jet tip velocity can produce the deeper penetration depth, this effect is likely not suitable for RLSC. This conclusion is drawn on the basis of data obtained during the experiments that though the wave shaper can control the detonation wave front and produce higher jet tip velocity, its penetration depth of RLSC with wave shaper is lower. Hence, it is a safe conclusion that the initiation delay time is the primary determinant of the penetration depth of RLSC.

In Figs. 14 and 15,  $t_0$  refers to the time when the reactive jet reaches the upper surface of steel plate, which increases with the increase of standoff, so the effective penetration time will decrease gradually. Consequently, for the RLSC with wave shaper, the

penetration depth decreases as the standoff increases from 0.5 to 1.5 CD. Especially, when the standoff is 1.5 CD, the effective penetration time is only about  $15 \mu s$ , resulting in the penetration depth dropping off significantly. For the RLSC without wave shaper, the penetration depth decreases first and then slightly increases with increasing the standoff. This may arise for two reasons: one is that the effective penetration time and the jet tip velocity are larger at 0.5 CD, and the other is that the reactive jet penetrator is longer at 1.5 CD. Moreover, as a result of the decrease of the initiation delay time of reactive jet with wave shaper, the penetration depths are smaller than that without wave shaper. In particular, with the increase of standoff, such deviation becomes larger. The first and most important reason is that, when the standoff is smaller, the tip velocity of reactive jet with wave shaper is much higher than that without wave shaper, which will have a significant advantage to penetration depth. Another important thing to be considered is that, when the standoff is larger, the effective jet velocity that involved in the penetration effects will decrease drastically (see Fig. 15 (b)) due to most part of reactive jet head with chemical reaction, which also leads the penetration depth to decrease. The last but important reason is that, when the standoff is 1.5 CD, the effective penetration time of reactive jet with wave shaper is much

less than that without wave shaper, which will cause a remarked reduction in penetration depth.

Furthermore, compared with the characteristics of reactive jet with and without wave shaper (see in Figs. 13 and 14), it is apparent that the mass of the slug with wave shaper is relatively larger, whereas its diameter of jet head is smaller than that without wave shaper. According to the Held.M radial expansion formula [36], the radius of penetration hole is proportional to the jet radius. As such, the entrance hole-diameters of reactive jet with wave shaper are all less than that of without wave shaper at the same standoff, as shown in Figs. 4 and 6.

In addition, the enhanced structural damage effects of the RLSC against steel plates are remarkably influenced by the effective mass of reactive materials into the penetration hole [4]. For the RLSC without wave shaper, the effective mass of reactive jet decreases with the increase of standoff. The main reason is that when standoff is smaller, the jet is not stretched enough, forming a short and thick cone penetrator, which leads to a higher mass per unit length inside the penetration hole. When the standoff is 0.5 and 1.0 CD, due to the more effective mass of reactive jet, the pressure produced by the deflagration of reactive materials is much greater than the yield limit of the steel plate, which would lead the steel plates to split into two fragments or form many large cracks, as shown in Fig. 5. However, for the RLSC with wave shaper, due to the thinner diameter of jet head and the shorter initiation delay time of reactive materials, the effective mass of reactive jet inside the penetration hole is too little to produce enough pressure to fracture the steel plate or even form a few small cracks (see in Fig. 3).

The higher temperature inside reactive jet is primarily responsible for the initiation delay time decrease if temperature induced initiation is assumed. Once the reactive jet initiates, it will heat the surrounding materials to the initiation threshold temperature and cause more deflagration during jet formation phase, resulting less deflagration inside the penetration hole, which will decrease the enhanced structural damage effects of the reactive liner shaped charge warheads. Hence, when a new reactive liner shaped charge warhead is considered, the temperature inside reactive jet should be controlled as much as possible so that the reactive materials chemical reaction is not occurring during jet formation to a larger extent, which will increase the initiation delay time of reactive jet and further eventually enhance its penetration behavior.

#### 4. Conclusions

The effect of wave shaper on penetration performance of RLSC against steel plates was studied. Several conclusions are presented as follows:

- Significantly differing from the wave shaper effect on traditional metal liner shaped charge, a negative effect of wave shaper on penetration performance of RLSC was revealed, including smaller hole diameter, lower penetration depth, and much less structural damage effects against steel plates.
- The negative effect of wave shaper on penetration performance of RLSC strongly depended on the standoff, showing a significant increase with increasing the standoff. Generally, when the standoff was higher than 1.0 CD, the penetration depth dropped off enormously.
- For mechanism considerations, when embedded a wave shaper in charge, the detonation waves superposition at the top of reactive liner produced an extreme overpressure zone, which dramatically increased the temperature inside reactive jet and decreased the initiation delay time of reactive jet, resulting in remarkably decreasing penetration performance and structural damage effects of steel plates.

#### Acknowledgments

The research was funded under the National Natural Science Foundation of China (No. U1730112), and supported by the State Key Laboratory of Explosion Science and Technology, Beijing Institute of Technology.

#### References

- DE Technologies. Inc. Reactive fragment warhead for enhanced neutralization of mortar, rocket, and missile threats. ONR-SRIR. 2006. p. 1–7. N04-903, <http://www.detc.com>.
- Daniels AS, Baker EL, DeFisher SE, et al. Bam bam: large scale unitary demolition warheads. In: 23rd international symposium on ballistics, Tarragona, Spain, April 16–20; 2007.
- Xiao JG, Zhang XP, Wang YZ, et al. Demolition mechanism and behavior of shaped charge with reactive liner. *Propellants Explos Pyrotech* 2016;41:612–7.
- Guo HG, Zheng YF, Yu QB, et al. Penetration behavior of reactive liner shaped charge jet impacting steel plates. *Int J Impact Eng* 2019;126:76–84.
- Lee RJ, Mock Jr W, et al. Reactive materials studies. Shock compression of condensed matter. 2005. p. 169–74.
- Hunt EM, Malcolm S, Pantoya ML, et al. Impact ignition of nano and micron composite energetic materials. *Int J Impact Eng* 2009;36:842–6.
- Ge C, Dong YX, Maimaitituersun W, et al. Experimental study on impact-induced initiation thresholds of Polytetrafluoroethylene/Aluminum composite. *Propellants Explos Pyrotech* 2017;42:514–22.
- Raftenberg MN, Mock W, Kirby GC. Modeling the impact deformation of rods of a pressed PTFE/Al composite mixture. *Int J Impact Eng* 2008;35:1735–44.
- Wang YZ, Yu QB, Zheng YF, et al. formation and penetration of jets by shaped charges with reactive materials liners. *Propellants Explos Pyrotech* 2016;41:618–22.
- Baker EL, Daniels AS, Ng KW, et al. Barrie: a unitary demolition warhead. In: 19th international symposium on ballistics, Interlaken, Switzerland; 23–27 May 2001.
- Xiao JG, Zhang XP, Guo ZX, et al. Enhanced damage effects of multi-layered concrete target produced by reactive materials liner. *Propellants Explos Pyrotech* 2018;43:955–61.
- Pazienza G. Calculation of the wave shaper effects on detonation wave in shaped charge. *Propellants Explos Pyrotech* 1987;12(4):125–9.
- Sachdeva SS, Bhattacharyya A, Kishore P, et al. Study on some aspects of performance of hollow charge. In: 17th International symposium on Ballistics, Midrand, South Africa, vol II; 1998. p. 299–306.
- Zhang Y, Zhang XF, He Y, et al. Detonation wave propagation in shaped charges with large wave-shaper. In: 27th international symposium on ballistics, Freiburg, Germany, April 22–26; 2013. p. 770–82.
- Xing BY, Liu RZ, Guo R, et al. Influence of the embedded structure on the EFP formation of compact terminal sensitive projectile. *Defence Technol.* 2017;(13):310–5.
- Naem Khalid, Hussain Arshad. Numerical and experimental study of wave shaper effects on detonation wave front. *Defence Technol.* 2018;(14):45–50.
- Zhu CS, Huang ZX, Zu XD, et al. Mach wave control in explosively formed projectile warhead. *Propellants Explos Pyrotech* 2014;39:909–15.
- Ding LL, Tang WH, Ran XW. Simulation study on jet formability and damage characteristics of a low-density material liner. *Materials* 2018;11:72.
- Hunt EM, Malcolm S, Pantoya ML, et al. Impact ignition of nano and micron composite energetic materials. *Int J Impact Eng* 2009;36:842–6.
- Wang HF, Zheng YF, Yu QB, et al. Impact-induced initiation and energy release behavior of reactive materials. *J Appl Phys* 2011;110:074904.
- Xu FY, Yu QB, Zheng YF, et al. Damage effects of double-spaced aluminum plates by reactive materials projectile impact. *Int J Impact Eng* 2017;104:13–20.
- Zhang XF, Shi AS, Zhang J, et al. Thermochemical modeling of temperature controlled shock-induced chemical reactions in multifunctional energetic structural materials under shock compression. *J Appl Phys* 2012;111:123501.
- Richard G. Ames. Energy release characteristics of impact-initiated energetic materials. In: Proceedings of materials research society symposium. Boston: Materials Research Society; 2006. p. 0896-H03-08.1-10.
- Richard G. Ames. Vented chamber calorimetry for impact initiated energetic materials. In: 43rd AIAA Aerospace sciences meeting and exhibit. Reno: Nevada; 2005. p. 279.1-3.
- Ge C, Dong YX, Maimaitituersun W, et al. Experimental study on impact-induced initiation thresholds of Polytetrafluoroethylene/Aluminum composite. *Propellants Explos Pyrotech* 2017;42:514–22.
- Cai J, Walley SM, Hunt RJA, et al. High-strain, high-strain-rate flow and failure in PTFE/Al/W granular composites. *Mater Sci Eng A* 2008;472:308–15.
- Lee I, Reed R, Brady V, et al. Energy release in the reaction of metal powders with fluorine containing polymers. *J Therm Anal* 1997;49(3):1699–705.
- Osborne DT, Pantoya M I. Effect of al particle size on the thermal degradation of al/teflon mixtures. *Combust Sci Technol* 2007;179:1467–80.
- Taylor PA. Private communication. Albuquerque, NM: Sandia National Laboratories; 2007.

- [30] Rogers GFC, Mayhew YR. Thermodynamic and transport properties of fluids. Blackwell; 1995.
- [31] Li RJ, Zhang JH, Wang JB. Numerical simulation of the effect of wave shaper on shaped charge jet's performance. *J. Proj. Rockets Missiles Guidance* 2012;32(3):107–10.
- [32] Kennedy JE. The gurney model of explosive output for driving metal. Explosive effects and applications. New York: Springer; 1998. p. 221–57.
- [33] Cao BY, Lassilab DH, Schneider MS, et al. Effect of shock compression method on the defect substructure in monocrystalline copper. *Mater Sci Eng* 2005;409. 270–409281.
- [34] Gang Tao, Hao Chen, Qincan Shen. Superplastic flow problems of copper shaped—charge jets. *Explos Shock Wave* 2008;28(4):336–40.
- [35] Losada M, Chaudhuri S. Theoretical study of elementary steps in the reactions between aluminum and teflon fragments under combusive environments. *J Phys Chem A* 2009;113(20):5933–41.
- [36] Held M. Verification of the equation for radial hole growth by shaped charge jet penetration. *Int J Impact Eng* 1995;17(1–3):387–98.